Name of Journal: *Radiology Innovation*
Manuscript Type: Original Article

Locally advanced rectal cancer: an MRI radiomics study on lymph node re-evaluation after neoadjuvant chemoradiotherapy

Short title: An MRI radiomics model for lymph node re-evaluation of locally advanced rectal cancer

Xiaoyan Zhang, Haitao Zhu, Lin Wang, Xiaoting Li, Yanjie Shi, Huici Zhu, Qingyang Li, Yingshi Sun*

Key laboratory of Carcinogenesis and Translational Research (Ministry of Education/Beijing), Department of Radiology, Peking University Cancer Hospital & Institute, Hai Dian District, Beijing 100142, China

*Corresponding author: Yingshi Sun, Key laboratory of Carcinogenesis and Translational Research (Ministry of Education/Beijing), Department of Radiology, Peking University Cancer Hospital & Institute, No.52 Fucheng Road, Hai Dian District, Beijing 100142, China
Email: sys27@163.com

ABSTRACT

Objective: To develop and validate one optimal MR radiomics model for lymph node (LN) re-evaluation of locally advanced rectal cancer (LARC) after neoadjuvant chemoradiotherapy (NCRT).

Methods: Four hundred and seven patients with clinicopathologically confirmed LARC in Beijing Cancer Hospital were included in this study from July 2010 to June 2015. All patients received NCRT before surgery, and underwent T2WI and DWI before and after NCRT. These patients were chronologically divided in the primary cohort (300 patients) and independent validation cohort (107 patients). The predicting model was trained and validated using postoperative pathological findings as truth values. By using radiomics method, we extracted the features of the tumor and the largest LN before and after neoadjuvant therapy, combined different features of the tumor and /or the largest LN before and/or after neoadjuvant therapy, and constructed 4 different prediction models, compared the performance of four predicting models. The optimal conducted to determine the clinical usefulness of the radiomics nomograms by quantifying the net benefits at different threshold probabilities in the validation dataset.

Results: In the primary cohort, the radiomics signatures from 4 models provided an AUC of 0.637, 0.709, 0.753, 0.835, respectively in LN re-evaluation after chemoradiotherapy. The diagnostic efficacy of model 4 was much better than that of 1, 2 and 3 model. In the validation cohort, the radiomics signatures provided an AUC of 0.795 for LN re-evaluation after chemoradiotherapy. The sensitivity, specificity, positive predictive value, negative predictive value were 0.813, 0.693, 0.531, 0.897, respectively (95% CI: 0.694 to 0.896, 0.647 to 0.911, 0.582 to 0.786, 0.361 to 0.621, 0.792 to 0.952). While the probability of predicting N+ ranges from 17% to 80%, using the proposed radiomics model to predict N+ shows a greater advantage than either the scheme in which all patients were assumed to N+ or the scheme in which all patients are N–. Decision curve analysis demonstrated that the radiomics nomograms were clinically useful.

Conclusion: With a systematic analysis and comparison of both pre-and post-NCRT MRI data, we constructed an optimal individualized LN re-evaluation model based on MR radiomics, combing primary tumor and the largest LN features, compared with other models (only with pre/post tumor or pre/post largest LN features).

Key words: Rectal neoplasms; Radiomics; Lymph node, re-evaluation; Neoadjuvant therapy

INTRODUCTION

Neoadjuvant chemoradiotherapy (NCRT) combined with total mesorectal excision (TME) is the current standard procedure for locally advanced rectal cancer (LARC).[1] After the completion of NCRT and before surgery, the primary tumor and lymph nodes should be re-evaluated to determine the therapeutic effect for further follow-up treatment plan.[2,3] At present, there is no characteristic radiologic sign or index accurately reflecting lymph node metastasis, so the efficiency of lymph node re-evaluation by imaging examination is not satisfactory.[4,5] Magnetic resonance imaging (MRI) has been widely regarded as an optimal diagnostic tool for clinical evaluation of rectal cancer, which can display the primary tumor, reveal the status of mesorectal fascia (MRF) and extramural venous invasion (EMVI).[6–10] and also demonstrate the distribution of lymph nodes (in and out of mesorectal fascia). Radiologists comprehensively determine whether lymph nodes are malignant by their size, shape, rim and signal intensity.[11,12] However, this diagnostic system highly depends on radiologists' experience which results in poor interobserver repeatability. DWI and ADC values were introduced to evaluate lymph node status, yet the diagnostic efficiency was not prominently improved.[13,14] Besides, lymph node (LN) re-evaluation is further complicated with chemoradiotherapy induced fibrosis, desmoplastic reaction, and colloid response.[15] Huang *et al*.[16] adopted the radiomics method based on CT imaging to evaluate the lymph node status of colorectal cancer, which showed the promising result. In the present study, we established different models with clinical information and radiomics features extracted from the primary tumor and/or the largest lymph node before and/or after NCRT in morphological (T2WI) and functional imaging (DWI) to predict lymph node metastasis. Among them, one optimal model was selected and validated by a new dataset. The aim was to assess the value of MRI-based radiomics model in LN re-evaluation of LARC after NCRT.

MATERIALS AND METHODS

Patient

Patients with clinicopathologically confirmed LARC in Beijing Cancer Hospital and who met the inclusion criteria between July 2010 to June 2015 were retrospectively enrolled in this study. The inclusion criteria were: (1) biopsy-proven primary rectal cancer; (2) LARC (T3-4 and/or N+) determined by pretreatment MRI; (3) no history of treatment of the rectal tumor and received complete NCRT in our institute;(4)

underwent TME after NCRT and had complete pathological information; (5) pre- and post-CRT MRI, including high resolution T2WI and DWI. The exclusion criteria were: (1) MRI quality was insufficient for measurements (e.g. movement artifacts); (2) mucinous adenocarcinoma confirmed by pathological results.

In total, 407 patients were enrolled, including 257 males and 150 females, with a mean (SD) age of 56 (11) years ranging from 21 to 87 years. From July 2010 to July 2014, patients were grouped into the primary cohort for feature selection, model development, and cross validation. Of these 300 patients, there were 182 males and 118 females, with a mean (SD) age of 55 (11) years ranging from 21 to 87 years. From August 2014 to June 2015, 107 patients were grouped into the independent validation cohort to test the generalization ability of the predicting model, including 75 males and 32 females, with a mean (SD) age of 59 (10) years ranging from 23 to 81 years.

MRI protocol

All patients received MRI examinations at two time points: within one week before the initiation of NCRT and within one week before surgery, which were defined as pre-NCRT MRI and post-NCRT MRI, respectively. MRI was performed with a 1.5-T or a 3.0-T scanner (GE Healthcare, USA) using an 8-channel phased array body coil in the supine position. To inhibit colonic motility, 20 mg of scopolamine butylbromide was intramuscular injected 30 min before scanning. Axial T2WI was also obtained using fat recovery fast spin echo and the acquisition parameters were as follows: repetition time (ms) / echo time (ms), 5694/110; field of view (FOV), 18.0 mm × 18.0 mm; matrix size, 288 × 256; echo train length, 24; section thickness, 3.0 mm; and intersection gap, 0.3 mm. DWI was obtained using a single-shot echo-planar imaging sequence, with a repetition time (ms) / echo time (ms) of 2800/70, 34.0 mm × 34.0 mm FOV, 256 × 256 matrix, 4.0-mm section thickness, 1.0-mm intersection gap, and 2*b* values (0, 1000 s/mm^2).

NCRT treatment

All patients received concomitant intensity-modulated radiation therapy (IMRT, 22 fractions of 1.8–2.0 Gy, total dose of 50.0–55.0 Gy)[17, 18] and simultaneous chemotherapy with capecitabine (825 mg/m^2/bid, oral administration). Eight to eleven weeks after the completion of NCRT, the patients underwent TME surgery.

Pathologic assessment

All specimens were assessed in accordance with the TNM staging system (American Joint Committee on Cancer, Cancer Staging Manual. 7th edit.) The predicting model was trained and validated using postoperative pathological findings as truth values. If there was any metastatic LN, the result was recorded as 1; otherwise, as 0.

Radiological assessment

MRI images were assessed by 2 senior radiologists who were blinded to any clinical or pathologic information.

Subjective evaluation of LN status

According to Beets-Tan and Beets,[4] LN status is determined comprehensively by their short axis (SA) and morphological features. Suspicious features for LN metastasis include irregular rim, heterogeneous signal intensity, and round shape. Specifically, LNs whose SA < 5 mm with all three suspicious features, LNs whose SA between 5 and 9 mm with two of the above three features, and LNs whose SA ≥ 9 mm with or without suspicious features are considered as metastatic LNs.

Conventional characteristics

The evaluated conventional characteristics of rectal cancer included tumor location, distance from the tumor inferior margin to the anorectal junction and to the anal verge, maximum tumor length and invasion depth (measured on oblique axial T2WI), extramural depth of tumor invasion (measured on oblique axial T2WI), distance from the deepest position of tumor invasion to circumferential resection margin (CRM, measured on oblique axial T2WI; if the distance was further than 1mm, CRM status was considered as negative, otherwise, positive), total number of visible LNs on MRI (combined axial T2WI and DWI); short axis of the largest LN (measured on axial T2WI).

Tumor masking

Regions of interest (ROIs) were manually delineated on pre- and post-NCRT T2WI and DWI (b = 1 000 s/mm^2), covering the entire tumor area in each consecutive slice. When there was no tumoral signal on the post-NCRT T2WI or DWI, free-hand ROIs were

drawn contouring the rectal wall at the former location of primary tumor according to the pre-NCRT examination.

LN masking

ROIs were delineated to cover the largest lymph node in T2WI in each consecutive slice.

Automate feature extraction

Radiomics features were extracted automatically from the tumor and the largest LN on T2WI before and after NCRT respectively, using an iN–house software programmed with MATLAB (R2011b，MathWorks). A total of 41 radiomics features were extracted, including 9 first-order gray level histogram features (maximum value, minimum value, median value, sum, mean value, variance, standard deviation, skewness and kurtosis), 24 gray level co-occurrence matrix (GLCM) texture features (energy, entropy, correlation, contrast, homogeneity, variance, sum mean, inertia, cluster shade (CS), cluster tendency (CT), max probability (MP), inverse variance (IV)), d =1 and 2) and 8 geometric features (volume, major axis length a, minor axis length b, eccentricity, elongation, orientation, volume of bounding box, perimeter), were acquired from each tumor or LN. The CT and IV were calculated. The long axis direction is defined as the angle between the long axis of the ellipse with the same moment of inertia as the largest section of the ROI and the horizontal direction. Extensibility is defined as the aspect ratio of the smallest rectangle where the largest section of the ROI is located. Functional features were extracted from the tumor before and after NCRT, including maximum, minimum, and average ADC values.

Development and validation of the predicting model

The least absolute shrinkage and selection operator (LASSO) was conducted to select the optimized subset of features and to calculate the radiomics score (Rad-score) of each patient.[19] In LASSO algorithm, the coefficients of some features are reduced to zero by adjusting the hyperparameter λ to select features. The 10-fold cross-validation (the sample was randomly divided into 10 portions, 9 for training and 1 for validation) was used to tune the hyperparameter λ by maximizing the area under curve (AUC) of receiver operating characteristic (ROC) curve. A radiomics score (Rad-score) was

calculated for each patient via a linear combination of selected features that were weighted by their respective coefficients.

To investigate the necessity of combining tumor and LN features from pre- and post-NCRT MRI, we established the following four models by their source: (1) tumor features + conventional measurements from post-NCRT MRI; (2) the largest LN features + conventional measurements from post-NCRT MRI; (3) tumor features+ the largest LN features + conventional measurements from post-NCRT MRI; (4) tumor features+ the largest LN features + conventional measurements from pre- and post-NCRT MRI. First, Bootstraps with 1000 resamples were used in the above 4 models and constructed 4 predicting models. The AUC, sensitivity (SEN), specificity (SPE), positive predictive value (PPV), and negative predictive value (NPV) were calculated to assess the performance of the predicting model in the primary cohorts. Then the optimal one was validated in an independent validation dataset.

Statistical analysis

All statistical analyses were performed using Statistical Package for the Social Sciences (SPSS) 22.0 (IBM Corp., Armonk, NY, USA). Two radiologists delineated ROIs and measured conventional characteristics of 80 consecutive patients (from June 2010 to December 2011) and calculated their Rad-score by using radiomics method independently. The intraclass correlation coefficients (ICC) were calculated to evaluate interobserver agreement (0.81–1.00 excellent, 0.61–0.80 good, 0.41–0.60 moderate, 0.21–0.40 fair, 0–0.20 poor). The independent-sample t test was used to compare the difference of continuous variable (age) between primary and validation cohorts. The Chi-square test was used to compare the dichotomous variables. And the independent sample t test was also applied to compare the difference between N+ and N– groups. $P < 0\ .05$ was considered as statistically significant.

Clinical use

Decision curve analysis was conducted to determine the clinical usefulness of the radiomics model by quantifying the net benefits at different threshold probabilities.[20]

RESULTS

Clinical characteristics

There was a significant difference in age between the primary and independent

validation cohorts. Other clinical and pathological characteristics, including gender, tumor location, and pathological lymph node status were not significantly different between the two groups (Table 1).

Table 1. Clinical and pathological characteristics of the primary and independent validation cohorts

Cohort	*n*	Gender		Age (year, $\bar{x} \pm s$)	Primary Site		Pathological N–stage	
		male	female		High, middle	low	N +	N −
Primary	300	182	118	55±11	83	217	80	220
validation	107	75	32	59±10	30	77	32	75
Test value		3.012[a]		3.108[b]	0.005[a]		0.415[a]	
P-value		0.083		0.002	0.169		0.730	

[a]Variables were tested using the χ^2 test. [b]Variables were tested using the *t*-test. N+: There was metastatic LN in the postoperative pathological finding. N–: There was no metastatic LN in the postoperative pathological finding.

Radiomics model construction and selection

The LASSO method tuned the hyperparameter λ corresponding to the maximum average AUC for feature selection (Figure 1). Fifteen features were selected with the hyperparameter λ = 0.024 from model 4, including 6 significantly different features between pathological LN-positive and negative groups (Table 2).

There was significant difference among the diagnostic efficacy in LN re-evaluation after NCRT of 4 models ($P < 0.01$, Table 3), in which model 4 was the optimal one with an AUC of 0.835 (Figure 2). Compared with the pathological truth value, the AUC of subjective LN re-evaluation after NCRT by 2 radiologists was 0.627 (95% confidence interval [CI]: 0.560–0.695) and 0.617 (95% CI: 0.549–0.685), respectively, which was significantly smaller than that of model 4 (Table 4).

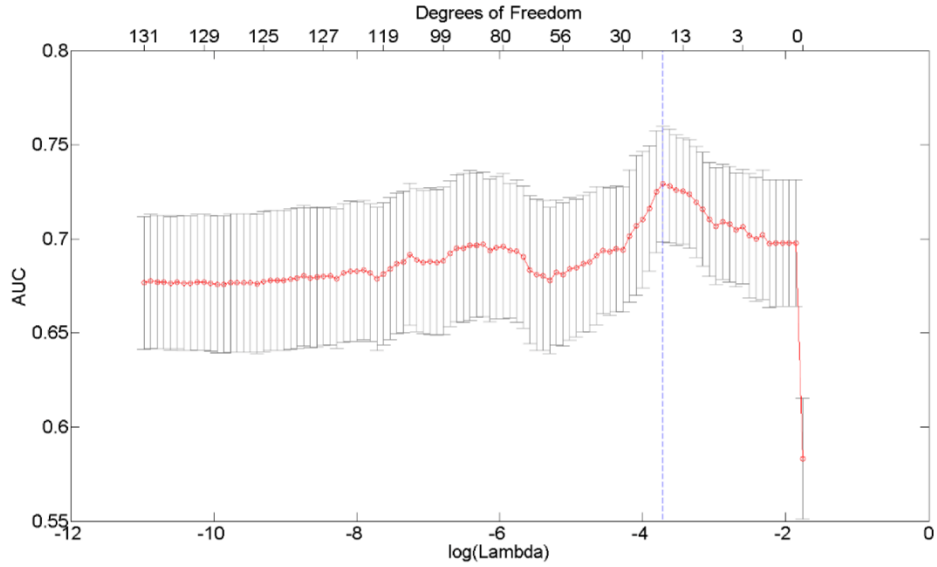

Figure 1. Radiomics feature selection using the least absolute shrinkage and selection operator (LASSO) of model 4 (tumor features+ the largest LN features+ conventional measurements from pre- and post-NCRT MRI). The vertical coordinate was the average area under the ROC (AUC) of the 10-fold cross-validation, the degree of freedom represented the selected feature number, the dotted line position was the log (λ) corresponding to the maximum AUC value, and the optimal λ was the λ corresponding to the maximum average AUC of the cross-validation. As the hyperparameter λ increased, the number of features selected by the model gradually decreased to 0. For each hyperparameter λ, the mean value of AUC obtained by 10-fold cross-validation was regarded as the variance. The LASSO method tuned the hyperparameter λ corresponding to the maximum average AUC for feature selection and removed unimportant features

Table 2. The weight coefficients of the selected features in model 4 in the primary cohort and the comparison results of each characteristic value between N+ and N– groups.

Feature	Weight	N– ($\bar{x} \pm s$)	N+ ($\bar{x} \pm s$)	Test Value	*P*-value
Post_LN_IntensityMin	–0.543	0.168±0.149	0.123±0.140	2.358	< 0.05
Post_LN_InverseVariance	1.899	0.289±0.145	0.399±0.194	4.625	< 0.01
Post_LN_Elongation	0.653	0.398±0.171	0.432±0.147	1.578	0.116
Post_LN_Orientation	–0.350	0.515±0.311	0.438±0.276	1.963	0.051
Post_Tumor_Elongation	5.794	0.091±0.023	0.104±0.048	2.272	< 0.05

Post_Tumor_ADCmin	-0.193	0.875±0.130	0.847±0.145	1.623	0.106
Post_Tumor_PrimarySite	-0.319	0.7621±0.258	0.700±0.274	1.816	0.070
Pre_LN_MinAL	5.470	0.214±0.081	0.321±0.173	5.310	<0.01
Pre_Tumor_Variance	1.101	0.030±0.064	0.055±0.154	1.413	0.161
Pre_Tumor_Tendency	-2.867	0.131±0.101	0.103±0.042	3.409	<0.01
Pre_Tumor_ADCmin	0.201	0.886±0.140	0.903±0.103	0.996	0.320
Pre_Tumor_ADCmean	0.891	0.374±0.138	0.390±0.113	0.883	0.378
Pre_Tumor_InvadedLength	-1.406	0.303±0.152	0.277±0.115	1.587	0.114
Pre_Tumor_INvadedDepth	-1.921	0.206±0.132	0.173±0.073	2.744	<0.01
Pre_Tumor_IDTMP*	0.069	0.308±0.118	0.328±0.161	1.001	0.319

N+: There was metastatic LN in the postoperative pathological finding. N–: There was no metastatic LN in the postoperative pathological finding. *IDTMP stands for invaded distance through the muscularis propria.

Table 3. The diagnostic efficiency of four models for predicting pathologic LN metastasis after NCRT in the primary cohort.

Model	AUC	SEN	SPE	PPV	NPV
1	0.637 (0.585–0.655)	0.375 (0.257–0.862)	0.846 (0.359–0.953)	0.469 (0.270–0.514)	0.788 (0.760–0.859)
2	0.709 (0.671–0.726)	0.625 (0.444–0.802)	0.718 (0.537–0.893)	0.446 (0.353–0.555)	0.840 (0.805–0.877)
3	0.753 (0.700–0.765)	0.688 (0.460–0.770)	0.750 (0.637–0.939)	0.500 (0.397–0.658)	0.868 (0.818–0.883)
4	0.835 (0.773–0.840)	0.750 (0.552–0.850)	0.746 (0.654–0.938)	0.517 (0.437–0.701)	0.891 (0.843–0.920)

Model 1: tumor features + conventional measurements from post-NCRT MRI. Model 2: the largest LN features + conventional measurements from post-NCRT MRI. Model 3: tumor features+ the largest LN features + conventional measurements from post-NCRT MRI. Model 4: tumor features + the largest LN features + conventional measurements from pre- and post-NCRT MRI. Numbers in parentheses were 95% confidence intervals.

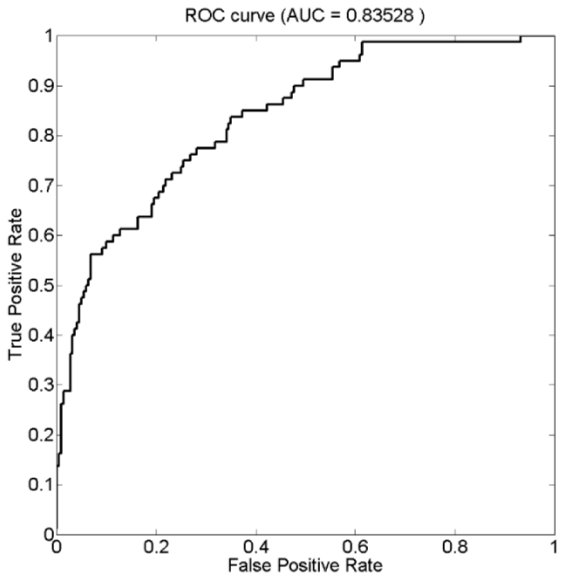

Figure 2. Receiver operating characteristic (ROC) curves of Rad-score calculated from model 4 for predicting LN metastasis compared with the pathological truth value. The area under the curve (AUC) value was 0.835.

Table 4. The diagnostic efficiency of two radiologists for subjectively predicting pathologic LN metastasis after NCRT in the primary cohort.

Rater	AUC	SEN	SPE	PPV	NPV
1	0.627 (0.560–0.695)	0.862 (0.770–0.922)	0.393 (0.330–0.459)	0.342 (0.281–0.433)	0.887 (0.808–0.936)
2	0.617 (0.549–0.685)	0.838 (0.742–0.903)	0.382 (0.322–0.450)	0.330 (0.280–0.409)	0.867 (0.804–0.934)

Numbers in parentheses were 95% confidence intervals. AUC: area under curve. SEN: sensitivity. SPE: specificity. PPV: positive predictive value. NPV: negative predictive value.

Interobserver agreement

Interobserver agreement was good to excellent for all the conventional characteristics between the 2 radiologists (ICC: 0.779–0.914, $P < 0.05$).

Independent validation of the radiomics model

As shown in Figure 3 and 4, the Rad-score was correlated with pathological LN status after NCRT. Specifically, if the Rad-score was positive, then the patient was considered as N+; if the Rad-score was negative, then the patient was considered as N–. In the independent validation cohort, the radiomics signatures provided an AUC of 0.795 for

LN re-evaluation after NCRT. The sensitivity, specificity, positive predictive value, negative predictive value were 0.813, 0.693, 0.531, and 0.897, respectively (95% CI: 0.694–0.896, 0.647–0.911, 0.582–0.786, 0.361–0.621, 0.792–0.952).

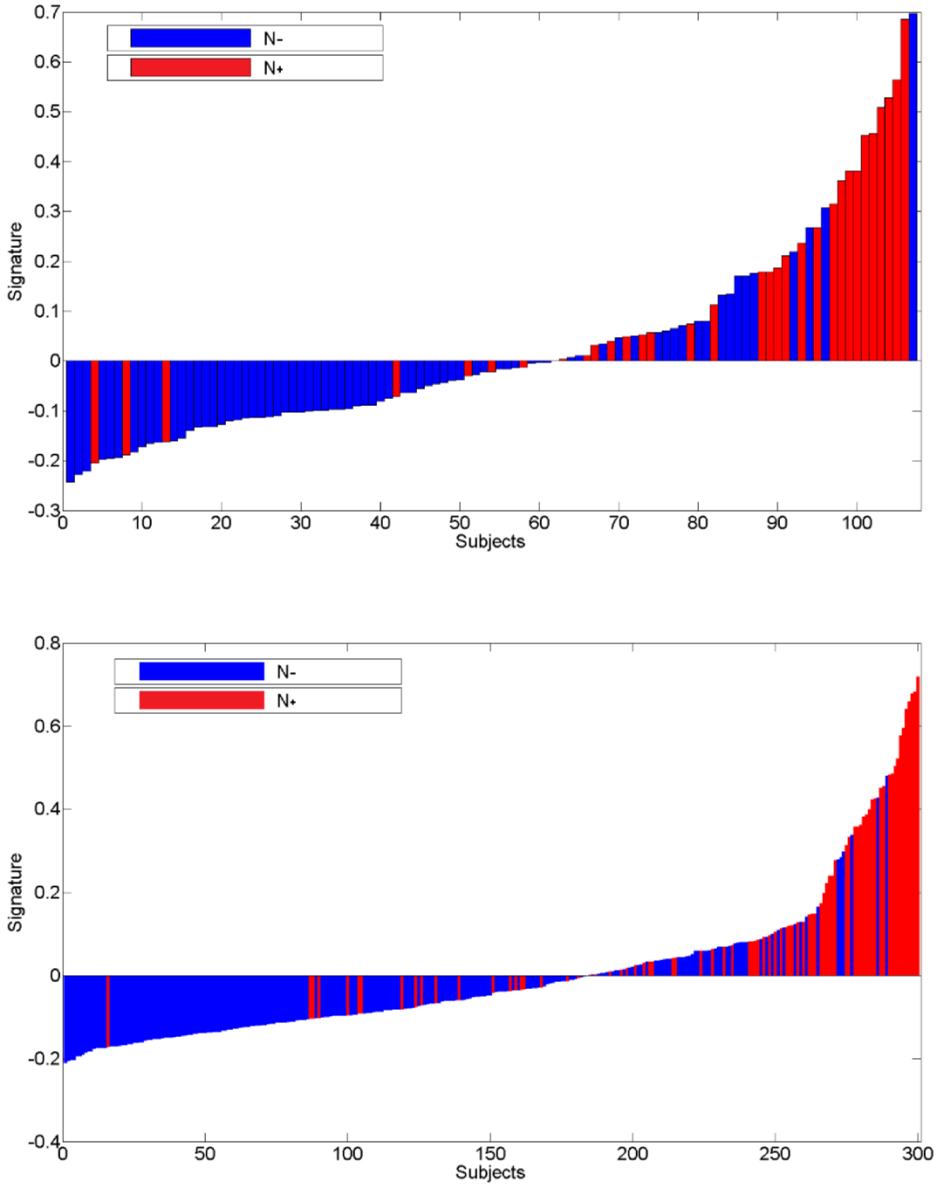

Figure 3, 4. Rad-score of model 4 in the primary cohort (Figure 3) and independent validation cohort (Figure 4) respectively. Red bars represented that there was metastatic LN in the postoperative pathological finding (N+), while blue bars represented no metastatic LN (N–). The higher the score, the more likely there existed metastatic LNs. Specifically, if the Rad-score was positive, then the patient was considered as N+; if the Rad-score was negative, then the patient was considered as N–.

Decision curve analysis

While the probability of predicting N+ ranges from 17% to 80%, using the proposed radiomics model to predict N+ showed a greater advantage than either the scheme in which all patients were assumed to N+ or the scheme in which all patients were N–. Decision curve analysis demonstrated that the radiomics nomograms were clinically useful (Figure 5).

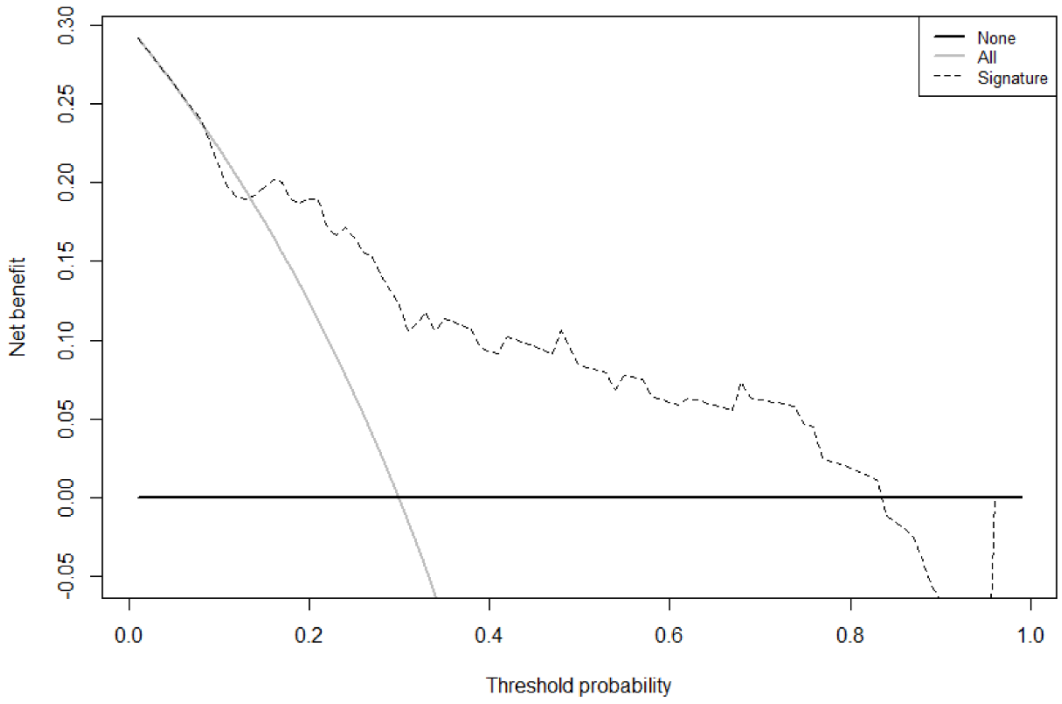

Figure 5. Decision curve analysis of model 4 in the independent validation cohort, quantifying the net benefits at different threshold probabilities. While the probability of predicting N+ ranges from 17% to 80%, using the proposed radiomics model to predict N+ showed a greater advantage than either the scheme in which all patients were assumed to N+ or the scheme in which all patients were N–.

DISCUSSION

The value of MRI-based radiomics predicting model for LN re-evaluation after NCRT in LARC

To re-evaluate LN status after NCRT, all patients enrolled in this study were diagnosed with locally advanced rectal cancer. Four different predicting models were constructed with factors closely related to LN status. Our study showed that LN status could not be evaluated accurately by radiomics features extracted from the tumor alone (model 1).

The LN status after NCRT is too complicated that simple replication of the LN evaluation model proposed by Huang *et al*.[16] is not appropriate. Besides, LN radiomics features alone (model 2) were not efficient for LN re-evaluation either. There were few factors included in the model even though LN radiomics features extracted from LN on post-NCRT MRI were correlated with pathological results more closely. Model 3 combined tumor radiomics features with LN radiomics features from post-NCRT MRI, achieving better diagnostic performance than model 1 and 2 did, with an AUC of 0.753. Given LN status after NCRT is affected by multiple factors in addition to the lymph node and tumor biological behavior,[21-23] we selected tumor and LN radiomics features from pre-NCRT MRI to reflect tumor burden in model 4, which remarkably outperformed the other 3 models.

By radiomics method, model 4 combined with all information available in routine clinical practice (including morphological / functional imaging information and tumor markers) to build a brand-new predicting model for LN re-evaluation of LARC after NCRT, whose diagnostic efficiency was also significantly superior to the conventional subjective LN evaluation (AUC: 0.627 and 0.617). The size, shape, rim and signal intensity can be recognized but cannot be quantitatively analyzed by naked eyes. With MRI-based radiomics method, not only visible information can be quantified avoiding the subjective bias of different observers, but also a large amount of digital information that cannot be recognized and distinguished by human eyes can be mined and integrated, thus improving the diagnostic efficiency of LN re-evaluation after NCRT.

Decision curve analysis demonstrated that while the probability of predicting N+ ranges from 17% to 80%, model 4 was clinically useful, superior to conventional LN evaluation. The main problem of this model is the low positive predictive value. However, false N positive would not lead to inadequate or delayed treatment for patients who routinely receive radical surgery after NCRT. While high negative predictive value of LN re-evaluation may result in treatment alteration, that is for true LN negative patients with T0 or T1-stage tumor, local excision could be implemented and anal sphincter function in patients with tumor located in the lower rectum could be preserved. Therefore, from the clinical perspective, accurate identification of patients with N0 is of greater clinical significance.

Limitations

Due to the retrospective study design, the lymph node couldn’t be matched lesion-by-

lesion from imaging to pathology, so an accurate N stage was not assessed in the present study. We selected the largest LN within the scanning coverage as one of the factors because on the patient level the larger the lymph node, the higher the probability of metastasis.[11, 12] It provided a new idea and method for retrospective study for LN re-evaluation after NCRT. We did not include the DWI information of LNs, and further analysis is needed to determine whether DWI is helpful for LN re-evaluation after NCRT. Besides, it was a retrospective study with single-center samples, our results should be prospectively evaluated and validated in prospective multicenter clinical trials.

In conclusion, with radiomics method, we explored the details of MRI images, including but not limited to lymph node size, shape, rim, internal signal intensity and other conventional characteristics for lymph node status evaluation, combined with morphological and functional information of the primary tumor, together with complete clinical data available in routine clinical practice of rectal cancer, and constructed an optimal individualized LN re-evaluation model after NCRT. Independent external validation results showed that the diagnosis efficiency of our model was better than the previous criteria, and clear clinical benefit can be achieved with it. Therefore, the application of this radiomics model can accurately predict the LN status after NCRT, and further realize personalized precision medicine.[24]

Source of Funding

National Natural Science Foundation of China (81641170); Special Clinical Application Research of Beijing (Z171100001017102).

Ethics Approval and Consent to Participate

This study was approved by the ethics committee of Beijing Cancer Hospital (ID. 2014KT89), and patient informed consent was waived due to its retrospective nature.

Conflict of Interests

None declared.

REFERENCES

1. Kapiteijn E, Marijnen CA, Nagtegaal ID, Putter H, Steup WH, Wiggers T*, et al.* Preoperative radiotherapy combined with total mesorectal excision for resectable rectal cancer. N Engl J Med 2001;345:638–646.

2. Schell SR, Zlotecki RA, Mendenhall WM, Marsh RW, Vauthey JN, Copeland EM, 3rd. Transanal excision of locally advanced rectal cancers downstaged using neoadjuvant chemoradiotherapy. J Am Coll Surg 2002;194:584–590; discussion 590–581.

3. Coco C, Manno A, Mattana C, Verbo A, Rizzo G, Valentini V*, et al.* The role of local excision in rectal cancer after complete response to neoadjuvant treatment. Surg Oncol 2007;16:S101–104.

4. Beets-Tan RG, Beets GL. Rectal cancer: review with emphasis on MR imaging. Radiology 2004;232:335–346.

5. Beets-Tan RG, Lambregts DM, Maas M, Bipat S, Barbaro B, Caseiro-Alves F*, et al.* Magnetic resonance imaging for the clinical management of rectal cancer patients: recommendations from the 2012 European Society of Gastrointestinal and Abdominal Radiology (ESGAR) consensus meeting. Eur Radiol 2013;23:2522–2531.

6. Beets-Tan RG, Beets GL, Vliegen RF, Kessels AG, Van Boven H, De Bruine A*, et al.* Accuracy of magnetic resonance imaging in prediction of tumour-free resection margin in rectal cancer surgery. Lancet 2001;357:497–504.

7. Bipat S, Glas AS, Slors FJ, Zwinderman AH, Bossuyt PM, Stoker J. Rectal cancer: local staging and assessment of lymph node involvement with endoluminal US, CT, and MR imaging--a meta-analysis. Radiology 2004;232:773–783.

8. Taylor FG, Quirke P, Heald RJ, Moran B, Blomqvist L, Swift I*, et al.* Preoperative high-resolution magnetic resonance imaging can identify good prognosis stage I, II, and III rectal cancer best managed by surgery alone: a prospective, multicenter, European study. Ann Surg 2011;253:711–719.

9. Li XT, Sun YS, Tang L, Cao K, Zhang XY. Evaluating local lymph node metastasis with magnetic resonance imaging, endoluminal ultrasound and computed tomography in rectal cancer: a meta-analysis. Colorectal Dis 2015;17:129–135.

10. Barbaro B, Vitale R, Leccisotti L, Vecchio FM, Santoro L, Valentini V*, et al.* Restaging locally advanced rectal cancer with MR imaging after chemoradiation therapy. Radiographics 2010;30:699–716.

11. Brown G, Richards CJ, Bourne MW, Newcombe RG, Radcliffe AG, Dallimore NS*, et al.* Morphologic predictors of lymph node status in rectal cancer with use of high-spatial-resolution MR imaging with histopathologic comparison. Radiology 2003;227:371–377.

12. Kim JH, Beets GL, Kim MJ, Kessels AG, Beets-Tan RG. High-resolution MR imaging for nodal staging in rectal cancer: are there any criteria in addition to the size? Eur J Radiol 2004;52:78–83.

13. Heijnen LA, Lambregts DM, Mondal D, Martens MH, Riedl RG, Beets GL*, et al.* DiffusioN–weighted MR imaging in primary rectal cancer staging demonstrates but does not characterise lymph nodes. Eur Radiol 2013;23:3354–3360.

14. Cho EY, Kim SH, Yoon JH, Lee Y, Lim YJ, Kim SJ*, et al.* Apparent diffusion coefficient for discriminating metastatic from noN–metastatic lymph nodes in primary rectal cancer. Eur J Radiol 2013;82:662–668.

15. Patel UB, Blomqvist LK, Taylor F, George C, Guthrie A, Bees N*, et al.* MRI after treatment of locally advanced rectal cancer: how to report tumor response--the MERCURY experience. AJR Am J Roentgenol 2012;199:486–495.

16. Huang YQ, Liang CH, He L, Tian J, Liang CS, Chen X*, et al.* Development and Validation of a Radiomics Nomogram for Preoperative Prediction of Lymph Node Metastasis in Colorectal Cancer. J Clin Oncol 2016;34:2157–2164.

17. Wang L, Li ZY, Li ZW, Li YH, Sun YS, Ji JF*, et al.* Efficacy and safety of neoadjuvant intensity-modulated radiotherapy with concurrent capecitabine for locally advanced rectal cancer. Dis Colon Rectum 2015;58:186–192.

18. But-Hadzic J, Anderluh F, Brecelj E, Edhemovic I, Secerov-Ermenc A, Hudej R*, et al.* Acute Toxicity and Tumor Response in Locally Advanced Rectal Cancer After Preoperative Chemoradiation Therapy With Shortening of the Overall Treatment Time Using Intensity-Modulated Radiation Therapy With Simultaneous Integrated Boost: A Phase 2 Trial. Int J Radiat Oncol Biol Phys 2016;96:1003–1010.

19. Tibshirani R. Regression shrinkage and selection via the lasso: a retrospective. Journal of the Royal Statistical Society Series B-Statistical Methodology 2011;73:273–282.

20. Vickers AJ, Elkin EB. Decision curve analysis: a novel method for evaluating prediction models. Med Decis Making 2006;26:565–574.

21. Coroller TP, Agrawal V, Huynh E, Narayan V, Lee SW, Mak RH*, et al.* Radiomic-Based Pathological Response Prediction from Primary Tumors and Lymph Nodes in NSCLC. J Thorac Oncol 2017;12:467–476.

22. Wu PQ, Liu ZY, He L. Perfect combination of radiomics and big data: the future of precision medical imaing. Chin J Radiol 2017;51:554–558.

23. Zhang LW, Fang MJ, Zang YL, Zhu YB, Dong D, Liu X*, et al*. Development and application of radiomics. Chin J Radiol 2017;51:75–77.

24. Balachandran VP, Gonen M, Smith JJ, DeMatteo RP. Nomograms in oncology: more than meets the eye. Lancet Oncol 2015;16:173–180.